

2D CFD Analysis of a Straight-bladed Vertical Axis Wind Turbine Using General Grid Interface Method

Farah Aqilah¹, Mazharul Islam^{*1}, Franjo Juretic², Waqar Asrar³

¹ Department of Mechanical and Production Engineering, Ahsanullah University of Science and Technology, 141 & 142, Love Road, Tejgaon Industrial Area, Dhaka-1208, Bangladesh

² Creative Fields Ltd., Dragutina Golika 63, 10000 Zagreb, Croatia

³ Department of Mechanical Engineering, International Islamic University Malaysia, 50728 Kuala Lumpur, Malaysia

ABSTRACT

Due to the ever-increasing need to lower the carbon pollution on earth, a method of generating electricity from kinetically-induced wind turbines is studied. Despite the commonly ventured horizontal axis wind turbine (HAWT), the vertical axis wind turbine (VAWT) has received increasing interest in the past decades due to its simple blade structures and small size. VAWT, specifically Straight-bladed vertical axis wind turbine (SB-VAWT) is one of the simplest types of VAWT for diversified applications. The winning factor against a normal HAWT is that they are relatively small in size and insensitive to incoming wind direction. In this study, the performance analysis of SB-VAWT is performed using the conventional Computational Fluid Dynamic (CFD) Model in two-dimension using the feature General Grid Interface (GGI) which can be found in the open-source CFD software, foam-extend v3.2. A transient solver with second order discretization scheme is used. The commonly used, $k-\omega$ SST turbulence model is applied in this study. The resulting power coefficient, C_p from the 2D CFD analysis is validated against experimental data. From the result, it is shown that the model under-estimate C_p value but closely matched with those from the experiment.

Keywords: Straight-bladed Vertical Axis Wind Turbine, fully turbulent model, $k-\omega$ SST, General Grid Interface, foam-extend.

1. Introduction

Demand for carbon emission reduction is high solely due to the effect of greenhouse gas emission and urbanization. The usage of wind turbines for electricity generation has increased over the years. It is in order to decrease the carbon dioxide pollution concentration in the atmosphere. The wind turbine is fundamentally a device to generate useful energy from kinetic energy stored in wind [1]. Most ventured wind turbines are the Horizontal Axis Wind Turbines (HAWT) which are mostly large in size and have complicated blade design. Due to these drawbacks, the interest in vertical axis wind turbine (VAWT) has emerged over the last couple of years. The advantages of VAWT over HAWT include smaller size, simpler blade design and more insensitivity to wind direction. Straight-bladed VAWT (SB-VAWT) is one of the simplest VAWT designs for diversified application. In the present study, a performance analysis of SB-VAWT is analysed using the conventional Computational Fluid Dynamics (CFD) model performed in two-dimensional domain. It is based on the reasoning that the flow profile around the straight blades can be considered two-dimensional, and allow for considerable savings in computational resources and simulation time.

Compared to the other numerical method such as the vortex model (namely vorticity transport model, VTM), momentum model (namely single streamtube model, the double-multiple streamtube model) or the cascade model[2], CFD provides the most detailed solutions of the Navier-Stokes equations[1].

In this study, the GGI (General Grid Interface) feature of foam-extend v3.2 [3] is used as sliding mesh method to interpolate solutions across boundary interfaces of different mesh regions [4]. It is similar to the Arbitrary Mesh Interface (AMI) [5] and is used for modelling of sliding mesh interfaces in turbomachinery's and SB-VAWT studies [6]. A comparative analysis has been done employing three different sliding mesh techniques namely AMI, GGI and Overset Methods for Dynamic Body Motions in OpenFOAM [7]. From the study, it is seen that the GGI sliding mesh method is marginally faster in parallel performance than other methods. This observation is also consistent among all cases tested. It is also shown that the GGI computations were able to run beyond large number of processors (i.e. 144 processors), whereas AMI computations show problems.

In the present study, a 2D CFD performance analysis of SB-VAWT is carried out in the employing a URANS based $k-\omega$ SST turbulence model with GGI sliding mesh method.

2. 2D CFD Analysis

The next subsection explains the process in detail.

2.1. Solid Modelling

A three-bladed, 2D solid modelling of SB-VAWT is prepared in STL format, developed in Blender. A traditional NACA 4-digit series airfoil, NACA0022 and a turbine diameter of 0.7 m are used in this study in order to match the experimental validation data from

* Corresponding author. Tel.: +88-01709300178

E-mail addresses: icmieekuet@gmail.com

[8]. The computational domain is divided into two parts: the stationary outer domain and the rotating inner domain as shown in Figure 1. The inner rotating domain, with diameter, $D=1\text{m}$, contains all three blades of SB-VAWT and rotates at a steady angular velocity of $\omega = 91.5\text{ rad/s}$ at the tip speed ratio, $\lambda = 4$, while being subjected to a wind velocity, V^∞ of 8 m/s at the inlet. The inner cylindrical rotating domain is connected to the stationary rectangular domain via a sliding mesh interface condition called General Grid Interface (GGI). The side walls of the domain are modelled as no-slip walls to mimic the wind tunnel conditions in ref. [8].

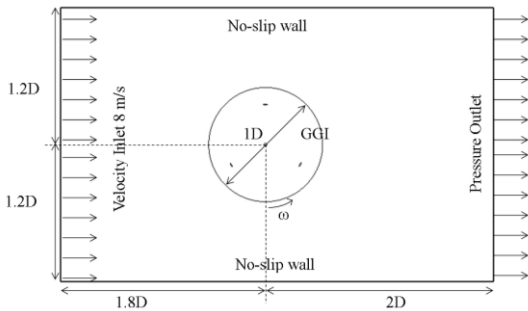


Fig.1 Computational domain of the study case with its boundary condition

2.2. Mesh Generation

An open-source meshing software, cfMesh[9] is used to generate mesh for the 2D simulations. The simulations are based on a structured-type mesh consisting of hexahedral and polyhedral grids. Mesh generations were done independently for stationary and rotating domains. The 2D mesh specifications are as follow:

- Number of cells: 132,546
- Growth rate: 1.2
- Maximum Aspect Ratio (AR): 1362.78
- Maximum mesh non-orthogonality: 53.06
- Maximum skewness: 2.76

Figure 2 shows the mesh of the inner domain. The mesh in the outer stationary domain is coarser compared to that of the rotor because the flow is mostly uniform there and therefore does not cause discretization errors. This reduces the simulation time and computational resources resulting in faster simulation run time. In contrast, the mesh in the inner rotating domain was made fine as it is where most wakes developed from rotor rotations. Mesh sensitivity analysis is carried out by changing the mesh size in the rotating domain only. In the near-blade area, 10 layers were generated to achieve y^+ value of less than 1, and accurately resolve the viscous effects in the boundary layers. As mentioned in ref. [10], 5 to 10 layers are encouraged to capture turbulence properties at the boundary layers. However, over-refining the mesh might results in the increase in round-off errors. Figure 3 and 4 show the mesh treatment of the SB-VAWT blade profiles.

GGI sliding mesh method is employed at the interface between rotating and static domain of SB-VAWT model. Due to the phenomenon of topological mesh changes which occurred typically when meshes of different dynamic motion is in used, a sliding grid interface is needed especially in the SB-VAWT study and other turbomachinery CFD analysis. The work of a sliding interface include detaching and attaching mesh connectivity on all cells and faces touching the sliding surface [11]. Detailed application of GGI feature is available in ref. [11].

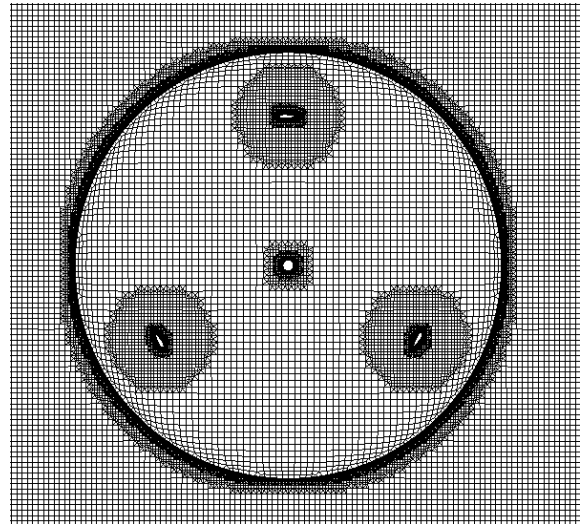


Fig. 2 Computational mesh of the rotating domain

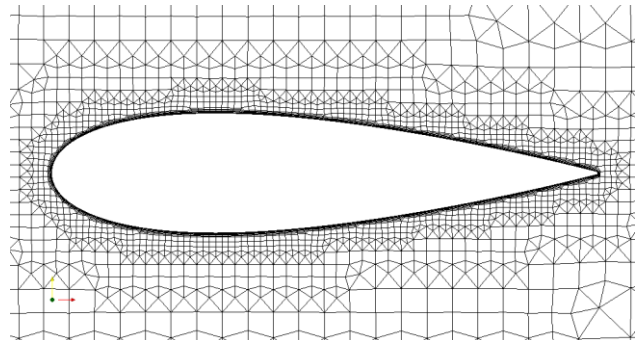


Fig. 3 Mesh around blade

2.3. Flow Solution

In order to solve the problem, the finite volume solver, foam-extend v3.2 is used. Foam-extend is a fork of OpenFOAM. The solution is produced using the Unsteady Reynolds Averaged Navier-Stokes (URANS) in order to take into account the unsteady effects of the simulations. A transient solver namely “pimpleDyMFoam” available in foam-extend is used. “pimpleDyMFoam” solves a dynamic motion fluid flow problem using the PIMPLE algorithm for pressure-linked equation. PIMPLE algorithm is available in OpenFOAM and foam-extend software

which consist of the combination of SIMPLE and PISO algorithms. A second-order linear UPWIND scheme is used to solve divergence parameters (U , k , ω , etc.), while pressure, p is solved using the second order Gauss scheme with linear interpolation scheme.

Turbulence modelling employed in this study is the commonly used k - ω Shear Stress Transport (SST) model by Menter et al including the implementation for wall functions. The header file for the application of the k - ω SST turbulence model in foam-extend is as of ref.

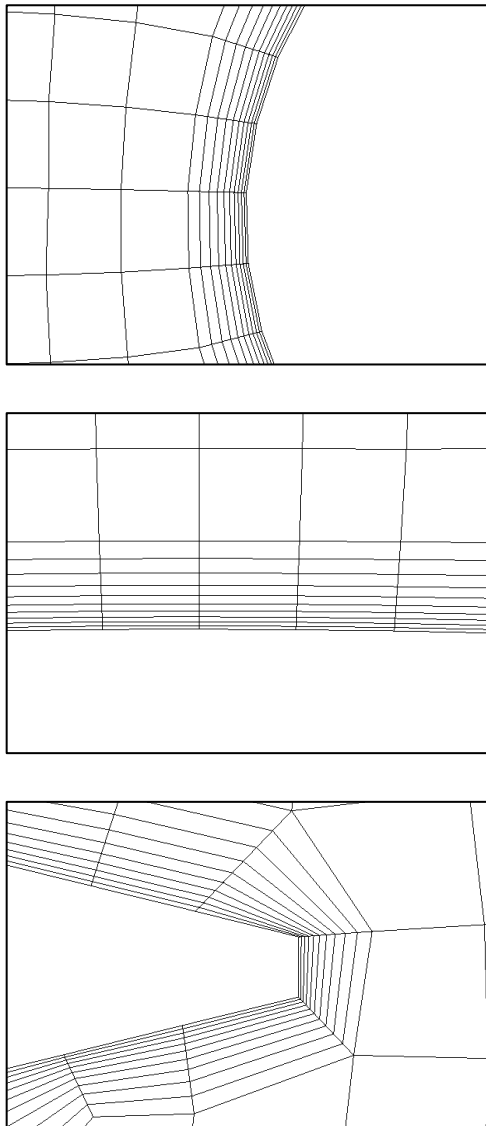


Fig. 4 10 layers mesh refinement at leading edge, middle and trailing edge of the rotor's blades

3. Results and Discussion

The results of the following CFD analysis are presented in this section.

3.1. Mesh Sensitivity Analysis

Mesh sensitivity analysis is important to achieve accurate CFD predictions. All numerical methods suffer from discretization errors such as the numerical dissipation produced by the blades of the rotors. These can be reduced by refining the computational grid. In practice, the large number of grids is often necessary to model the flow in the wake of the blade of SB-VAWT [1]. However, over-refining the mesh may result in the increase of round-off errors [10]. Thus, mesh sensitivity analysis is carried out to determine the mesh size resulting in mesh independent solution and consequently produces reliable results. Three different mesh refinement classes are prepared namely Coarse (M1), Medium (M2) and Fine (M3). The mesh consists of polyhedral and hexahedral cell generated using the open-source software, cfMesh. Table 1 show the quality metrics for each mesh refinements.

Table 1. Mesh descriptions for 2D CFD mesh sensitivity analysis

	Coarse (M1)	Medium (M2)	Fine (M3)
Number of cells	120 477	122 730	132 546
Growth Rate	1.2	1.2	1.2
Maximum Aspect Ratio (AR)	488.8	611.1	1362.7
Maximum Non-orthogonality	63.2	69.5	53.0
Maximum Skewness	2.4	2.7	2.7

The simulation on all three meshes were performed using Shear Stress Transport (SST) k - ω turbulence model and the same second order discretization scheme described above. In addition, all three cases were run using the same initial boundary conditions for one revolution of the rotor mesh. The resulting CP value from the following mesh refinements are recorded as in Figure 5.

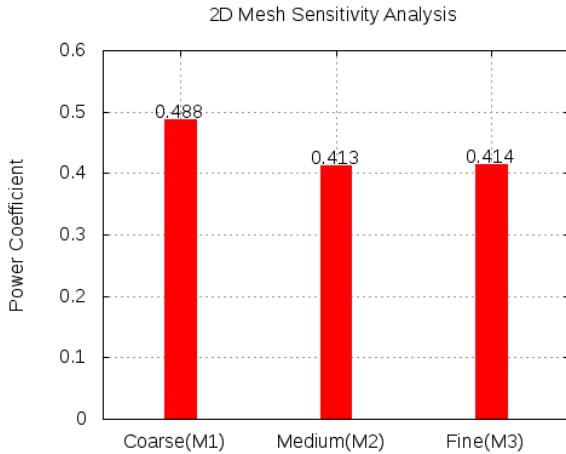


Fig. 5 C_p comparison for the three classes of mesh refinements

From the Figure 5, the mesh independency is achieved and the resulting C_p does not change significantly with further mesh refinement. Fine mesh (M3) is used for the final 2D analysis.

3.1. Experimental Validation

As mentioned before, the unsteady effect of the simulation is modelled by employing the URANS method and solving using a transient solver. Only one case of tip speed ratio, $\lambda = 4$ is carried out in this study. The simulation is ensured to reach convergence before calculating its C_p value. The periodic convergence is observed to be achieved after the 3rd revolutions as shown from the blade torque ripple in Figure 6. Tolerances for all parameters are set to 1×10^{-7} .

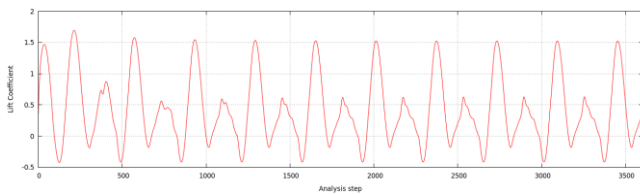


Fig. 6 Blade torque ripple for 10 revolutions

The power coefficient is then compared with those in . Figure 7 shows the final result of the power coefficient. The predictions of C_p from the CFD simulations have shown to under-estimate the experimental results by 27% due to errors. C_p value for a whole 10 revolutions of the simulation is 0.21 at $\lambda = 4$. This may happen due to the usage of a fully-turbulent model, $k-\omega$ SST.

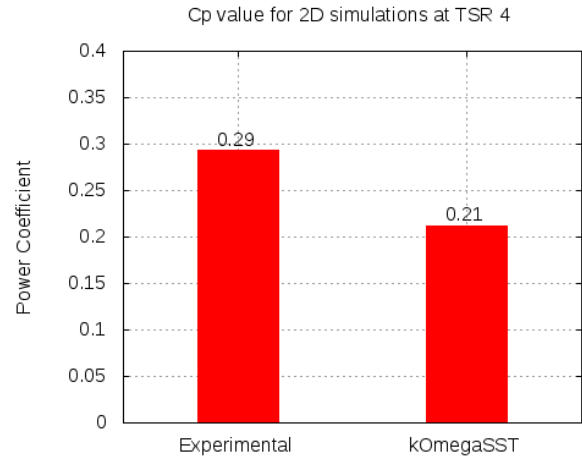


Fig. 7 C_p value for 2D simulations at $TSR = 4$

3.3. Contour Plot

Post-processing of the results is performed by using ParaView, the software used for generating of contour plots and gnuPlot to generate graphs. Figure 8 shows the blade torque at one revolution after convergence at $\lambda = 4$. The curve matched with good agreement to the curve in ref. . It can be seen that the highest predicted value of blade torque, T_b is in the upwind region approximately at azimuthal angle, $\theta = 80^\circ$ where the blade is subjected to flow of wind. At θ more than 180° , the T_b is slightly distorted due to wake disruption from other blades. Figure 9 shows the velocity field contour plot where wake resulting from blades occurred at the downwind region thus developed a low T_b . The phenomenon, denoted by the letter A, in the Figure 9 shows a discrepancy where simulations predict a low speed wake resulting in wake separation when blade enters the downwind region.

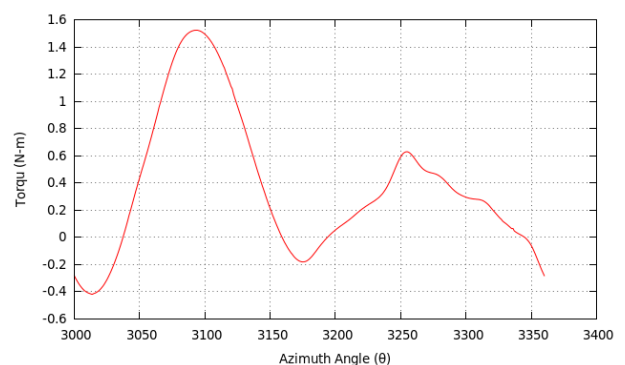


Fig. 8 Blade torque for 1 revolution at the end of 10th revolution versus azimuth angle, θ°

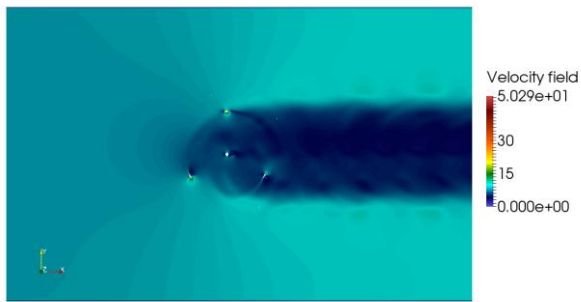


Fig. 9 Velocity field contour plot at the end of 10th revolution

Figure 10 shows the predicted vorticity contours at $\lambda = 4$. The blade enters the stall vortices created by other blade rotors, which is only detaching at almost when entering the downwind region. The shedding around the turbine show strong ripple at the downwind region pass central column where the developed vortices disrupt the performance of the rotors. Although the simulations predict a good agreement results when compared to experimental data in ref., the usage of transitional turbulence model instead of a fully-turbulent model is encouraged. From ref. , the author emphasize the importance of transitional turbulence model where the flow structures such as vortices and wake are highly mixed, thus prevent strong ripples to occur at the rotor area which is significantly similar to experimental measurements.

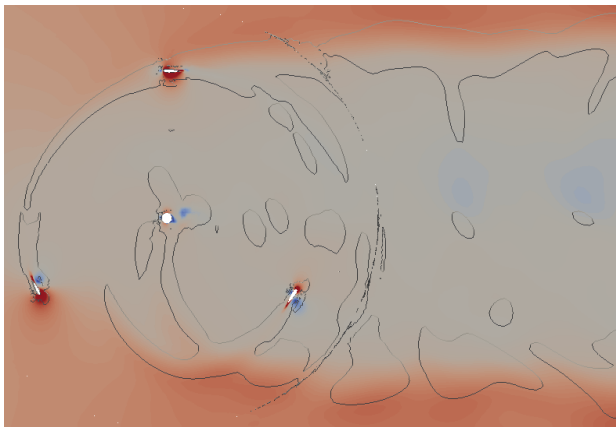


Fig. 10 Vorticity contours at TSR = 4 using k- ω SST model

4. Conclusions

Two-dimensional CFD model has been used to perform the flow analysis of a three-bladed SB-VAWT in this study. GGI has been applied at the interface between rotating and stationary domains. The resulting power

coefficient from the analysis agrees closely with the experimental data at the same operating conditions. The accuracy of flow predictions can be further improved by using the transitional turbulence model instead of the fully-turbulent model used in this study. The studied flow is in the transition regime where the tip speed ratio and the Reynolds Number are relatively low. Furthermore, the transition turbulence model namely the LCTM (γ - $Re_{\theta t}$) and LKE (k - k_L - ω) model handle the turbulence closure differently compared to the k - ω SST model.

Acknowledgements

Preparation of the article was supported by the Research Initiative Grant Scheme (RIGS) by the International Islamic University Malaysia (IIUM) funded by the Ministry of Higher Education (MOHE) Malaysia.

REFERENCES

- [1] Scheurich F.; and Brown R. E. (2011). The effect of dynamic stall on the aerodynamics of vertical-axis wind turbines. *29th AIAA Applied Aerodynamics Conference 2011*
- [2] Islam M.; Ting D.S. K.; Fartaj A. (2008). Aerodynamic models for Darrieus-type straight-bladed vertical axis wind turbines. *Renewable and Sustainable Energy Reviews*, 12, 1087–1109.
- [3] OpenFOAM (2002). The OpenFOAM® Extend Project. Retrieved December 5, 2015, from <http://www.extend-project.de/>.
- [4] Beaudoin M.; Jasak H. (2008). Development of a Generalized Grid Interface for Turbomachinery simulations with OpenFOAM. *Open Source CFD International Conference*.
- [5] Beatty S. J.; Mishra V.; Beatty S.; Buckham B.; Oshkai P.; and Crawford C. (2015). Application of an Arbitrary Mesh Interface for CFD Simulation of an Oscillating Wave Energy Converter Application of an Arbitrary Mesh Interface for CFD Simulation of an Oscillating Wave Energy Converter.
- [6] Lloyd T. P. (2011). The OpenFOAM Generalised Grid Interface. *University of Southampton* Retrieved March 30, 2017, from <https://cmg.soton.ac.uk/community/attachments/107/ggiPresentationLloydAug11.pdf>.
- [7] Chandar D.; and Gopalan H. (2016). Comparative Analysis of the Arbitrary Mesh Interface(AMI) and Overset Methods for Dynamic Body Motions in OpenFOAM. *46th AIAA Fluid Dyn. Conf.*, June, 1–12.
- [8] Danao L. A. (2012). The Influence of Unsteady Wind on the Performance and Aerodynamics of

Vertical Axis Wind Turbines. phdthesis, University of Sheffield, UK.

- [9] cfMesh (2002). cfMesh: Advance Meshing Tool. Retrieved June 25, 2016 from <http://cfmesh.com/>
- [10] Tu J.; Yeoh G. H.; and Liu C. (2013) *Computational Fluid Dynamics - A Practical Approach (2nd Edition)*. Elsevier.
- [11] Jasak H. (2009). General Grid Interface: Theoretical Basis and Implementation,” *Wikki Ltd, UK*. Retrieved March 30, 2017, from <http://powerlab.fsb.hr/ped/kturbo/OpenFOAM/SuimmerSchool2009/lectures/TurboGGI.pdf>.